Science of the Total Environment 918 (2024) 170662

Contents lists available at ScienceDirect

Science of the Total Environment

journal homepage: www.elsevier.com/locate/scitotenv

# New versus naturally aged greenhouse cover films: Degradation and micro-nanoplastics characterization under sunlight exposure

Carmen Sorasan [a], Patricia Taladriz-Blanco [b,c,*], Laura Rodriguez-Lorenzo [b], Begoña Espiña [b], Roberto Rosal [a]

[a] Department of Analytical Chemistry, Physical Chemistry and Chemical Engineering, University of Alcalá, Alcalá de Henares, E-28871 Madrid, Spain
[b] International Iberian Nanotechnology Laboratory (INL), Water Quality Group, Av. Mestre José Veiga s/n, 4715-330 Braga, Portugal
[c] Adolphe Merkle Institute, University of Fribourg, Chemin des Verdiers, 4, 1700 Fribourg, Switzerland

## HIGHLIGHTS

- MPLs and NPLs of PE were detected in water during the aging of LDPE greenhouse films.
- The polymeric structure of PE changes during the aging process.
- FC and TOC analyses revealed that materials other than PE were released during aging.
- Micro- and nanoplastic release differs between new and naturally aged plastics.

## GRAPHICAL ABSTRACT

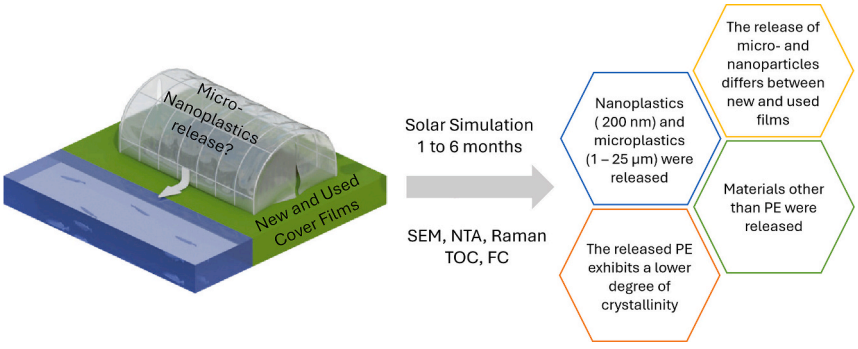


## ARTICLE INFO

Editor: Elodie PASSEPORT

*Keywords:*
Nanoplastics
Aging
Greenhouse
Raman spectroscopy
Nanoparticle tracking analysis

## ABSTRACT

The understanding of microplastic degradation and its effects remains limited due to the absence of accurate analytical techniques for detecting and quantifying micro- and nanoplastics. In this study, we investigated the release of nanoplastics and small microplastics in water from low-density polyethylene (LDPE) greenhouse cover films under simulated sunlight exposure for six months. Our analysis included both new and naturally aged (used) cover films, enabling us to evaluate the impact of natural aging. Additionally, photooxidation effects were assessed by comparing irradiated and non-irradiated conditions. Scanning electron microscopy (SEM) and nanoparticle tracking analysis (NTA) confirmed the presence of particles below 1 µm in both irradiated and non-irradiated cover films. NTA revealed a clear effect of natural aging, with used films releasing more particles than new films but no impact of photooxidation, as irradiated and non-irradiated cover films released similar amounts of particles at each time point. Raman spectroscopy demonstrated the lower crystallinity of the released PE nanoplastics compared to the new films. Flow cytometry and total organic carbon data provided evidence of the release of additional material besides PE, and a clear effect of both simulated and natural aging, with photodegradation effects observed only for the new cover films. Finally, our results underscore the importance of studying the aging processes in both new and used plastic products using complementary techniques to assess the environmental fate and safety risks posed by plastics used in agriculture.

* Corresponding author at: International Iberian Nanotechnology Laboratory (INL), Water Quality Group, Av. Mestre José Veiga s/n, 4715-330 Braga, Portugal.
*E-mail address:* patricia.taladrizblanco@unifr.ch (P. Taladriz-Blanco).

https://doi.org/10.1016/j.scitotenv.2024.170662
Received 14 December 2023; Received in revised form 22 January 2024; Accepted 1 February 2024
Available online 3 February 2024

## 1. Introduction

Greenhouse plastic cover films, typically composed of polyethylene (PE), have been shown to release microplastics (MPLs) into the environment during their usage (Gündoğdu et al., 2022b) These MPLs can subsequently enter the water environment through processes like leaching and stormwater runoff, thereby exacerbating concerns related to global climate change. (de Souza Machado et al., 2019; Gündoğdu et al., 2022a; Hitchcock, 2020; Owusu et al., 2024; Sharma et al., 2023) Plastic products, plastic waste, and primary MPLs can undergo degradation, forming small micro- and nanoplastics (NPLs) through a combination of biotic and abiotic processes. (Chamas et al., 2020; Liu et al., 2022) The definition of MPLs generally encompasses plastic particles with sizes below 5 mm, while NPLs are typically considered to be those with sizes below 1 μm. (Gigault et al., 2018; Hartmann et al., 2019) The biotic degradation of plastics involves the enzymatic breakdown of polymer chains by microorganisms such as bacteria, fungi, or algae, producing short-chain oligomers or monomers. In contrast, abiotic degradation of plastics occurs through mechanisms such as photodegradation, thermal degradation, and mechanical degradation, resulting in the formation of MPLs and NPLs, as well as short polymer chains, gases, and other small molecules as byproducts. (Zhang et al., 2021).

Photodegradation leading to the formation of small MPLs and NPLs has been documented in previous studies. (Gigault et al., 2016; Liu et al., 2022; Tong et al., 2022; Zhang et al., 2021) These studies have included the quantification of NPLs generated from MPLs of materials such as polystyrene (PS), polypropylene (PP), and low-density polyethylene (LDPE) under UV-light exposure, (Song et al., 2022) as well as the production of MPLs from LDPE films with varying degrees of crystallinity. (Cui et al., 2022) Additionally, Sorasan et al. (Sorasan et al., 2021, 2022) observed the generation of NPLs during the photo-aging of LDPE in water and marine plastic debris composed of PE, PP, and PS. At the same time, Song et al. (Song et al., 2020) detected MPLs and NPLs in weathered expanded PS boxes. Pfohl et al. (Pfohl et al., 2022) adapted the standardized NanoRelease protocol to quantify small MPLs and NPLs released from aged polyamide and polyurethane powders in water. Furthermore, there have been investigations into the release of MPLs and NPLs from various plastic products, including studies on MPLs released from teabags, (Hernandez et al., 2019) clothing during washing, (Wang et al., 2023) and coffee cups. (Ekvall et al., 2019) However, many of these studies do not consider the differential effects of aging on naturally aged (used) plastics compared to new ones.

MPLs and NPLs, resulting from the degradation of plastic products, can persist in the environment for years, causing pollution and posing risks to wildlife and humans. (Alimi et al., 2018) Their presence has been reported in various ecosystems including soil, (Astner et al., 2023; Li et al., 2024; Pérez-Reverón et al., 2023) as well as in food and beverages. (EFSA CONTAM Panel (EFSA Panel on Contaminants in the Food Chain), 2016; Allen et al., 2022; Belz et al., 2021; Gálvez-Blanca et al., 2023; Ivleva et al., 2017; Science for the Environment Policy, 2023) MPLs and NPLs differ from macro- and mesoplastics in their behavior and physicochemical properties. (Gigault et al., 2018; Science for the Environment Policy, 2023) Smaller plastic particles can easily penetrate biological barriers, translocate through different organs, and enter cells. Additionally, the high surface area-to-volume ratio makes NPLs more likely to adsorb significant amounts of other pollutants, release plastic additives, and interact with other molecules or materials in their surroundings. However, the detection and quantification of NPLs present significant challenges due to the lack of precise and accurate analytical approaches and techniques. (Caldwell et al., 2022; Ivleva, 2021) These challenges stem from their polydispersity in size and shape, hydrophobic nature, limited chemical reactivity, low predicted environmental concentrations and the complex matrices in which they are dispersed. (Gigault et al., 2021; Mitrano et al., 2021; Science for the Environment Policy, 2023) Separation and pre-concentration techniques such as density separation, elutriation, filtering/sieving, asymmetric flow field-flow fractionation, and cloud point extraction are commonly employed for MPLs and NPLs analysis. Raman spectroscopy, Fourier transform infrared spectroscopy (FTIR), and pyrolysis gas chromatography–mass spectrometry are the main techniques used for identification and quantification. However, the spatial resolution limitations of FTIR (10 μm) and Raman (100 μm – 1 μm for conventional Raman and 500 nm for confocal Raman), as well as the destructive nature of pyrolysis, restrict their applicability. Surface-enhanced Raman spectroscopy (SERS) has shown promise in overcoming these limitations, as it allows for the detection of small NPLs ($\leq$ 100 nm) using various plasmonic nanostructures. (Caldwell et al., 2021; Kihara et al., 2022; Lv et al., 2020).

To obtain a comprehensive understanding of the quantity and size distribution of particles that may be released into the water environment from the photodegradation of greenhouse LDPE cover films, we studied the degradation of both new and used LDPE greenhouse cover films over six months using well-established nano techniques. The greenhouse cover films were sourced from Almeria, Spain, where an area well over 30,000 ha is covered by greenhouses.(Castillo-Díaz et al., 2021) It is important to know that most vegetables grown in these greenhouses are sown and harvested within 6 months, underscoring the relevance of our work. Raman spectroscopy, electron microscopy and nanoparticle tracking analysis (NTA) were used to extract the chemical fingerprint, size and shape distribution, and concentration of the released plastic particles upon simulated sunlight exposure for six months. The results demonstrate the release of nanoparticles at all investigated time points. Of particular interest is the finding that the release of nanoparticles is only affected by the natural aging of the films. In contrast, the release of microplastics is influenced by both simulated and natural aging. Effects of photodegradation were observed only for the new-MPLs, and Raman results clearly showed that the smallest released LDPE particles exhibit a low degree of crystallinity.

## 2. Materials and methods

### 2.1. Sample preparation

Commercially available 5-sheet LDPE greenhouse cover films (Naturmax® 3 A, average thickness of 200 μm, duration according to the supplier: 3 years, Naturplás, El Ejido, Almeria) were cut in 5 mm × 5 mm MPLs pieces using scissors and stored in sealed polystyrene storage boxes before simulated sunlight exposure. LDPE MPLs (0.1 ± 0.01 g/mL) placed in a glass beaker were dispersed in 500 mL of ultrapure water (Milli-Q System, Millipore) and irradiated using an LCS-100™ solar simulator provided with a 100 W Xenon Lamp (Newport Corp, Model 94011 A) at ~ 18 cm from the output flange (corresponding to 1858 W $m^{-2}$ which is 10 times the solar irradiance). Under these conditions, 3 days of irradiation corresponds to ~ 1 month of average sunlight in the Iberian Peninsula (4.4 kWh $m^{-2}$ $day^{-1}$ or 183.33 W $m^{-2}$).(Sorasan et al., 2021) Due to the close proximity of the samples to the lamp, water evaporation was observed. Therefore, the beaker was refilled with Milli-Q water on demand to keep the volume of water constant during the exposure time. New and used LDPE MPLs were exposed to sunlight and analyzed. Non-irradiated samples were kept in the dark for the same time as the irradiated samples, i.e., up to 18 days and were used as controls. An additional control was included in the study to evaluate the release of particles, both from new and used LDPE MPLs (0.1 g/mL), at an early time point of 2 h in Milli-Q without irradiation.

### 2.2. Nanoparticle tracking analysis (NTA)

The presence of nanoparticles with diameters below 1 μm was evaluated by NTA using a Nanosight NS300 (Malvern) provided with a 488 nm CW laser (max. power < 55 mW). 1 mL of sample was analyzed using a flow-cell top plate made of glass and sealed with a PDMS ring, fluxed at a speed of 100, and imaged with a camera level and screen gain set at 12 and 8 (Slider Shutter = 1200; Slider Gain = 125), respectively.

The flow-cell top-plate was filled using 1 mL polypropylene syringes (Fisher Scientific). Five videos of 60 s each were recorded (total frames = 1498) and analyzed to obtain the size distribution and concentration of particles/mL for the different samples at room temperature. Unless otherwise specified, samples were analyzed without any pre-treatment step. Controls and Milli-Q water were analyzed using the same above-mentioned conditions. The chamber was cleaned thoroughly using Milli-Q water between sample analyses.

It is worth nothing that NTA relies on the scattering properties of the particles and their Brownian motion to determine their size (i.e. distribution) by applying the Einstein-Stokes equation. Unlike dynamic light scattering (DLS), which is commonly used to assess the size distribution of nanoparticles, NTA provides size values that are number-weighted. (Filipe et al., 2010) This characteristic reduces bias introduced by the presence of larger particles in the analysis. Furthermore, NTA provides information about the concentration of particles per mL and has been reported as a promising tool for characterizing polydisperse nanoparticles (including NPLs) in complex matrices. (Mehrabi et al., 2017) This capability is particularly relevant in the study of nanoparticles released from natural samples, as it allows discrimination of undesirable particles, and nanoparticles with different sizes in a polydisperse sample can be visualized by simply adjusting the camera level and the screen gain.

### 2.3. Flow Cytometry (FC)

The presence and concentration of particles with diameters in the 1 μm – 25 μm range were analyzed using a FACSCalibur flow cytometer (Becton Dickinson) following the experimental procedure followed elsewhere (Sorasan et al., 2021, 2022). Briefly, samples were filtered using a 100 μm stainless steel filter (CISA) and injected in the instrument previously calibrated using PS beads (Molecular Probes and Supelco) in the 1–25 μm size range. Intensity values were converted into particle size using scattering cross-sections derived from Mie's theory, as shown elsewhere. (Sorasan et al., 2021).

### 2.4. Total organic carbon (TOC) determination

The TOC was determined as non-purgeable organic carbon (NPOC) as described elsewhere using a Shimadzu TOC-VSCH apparatus equipped with an ASI-V autosampler.(González-Pleiter et al., 2019; Sorasan et al., 2022, 2021) Briefly, samples were filtered using a 1 μm pore size Puradisc 25 PTFE filter (Sigma-Aldrich) and injected into the instrument.

### 2.5. Scanning electron microscopy (SEM)

A FEI Quanta 650 FEG-ESEM equipped with secondary electron and backscatted electrons (SE/BSE) detectors (ThermoFisher) operating at 5 kV and high vacuum (spot size 3), was used to image the samples. 5 μL of the sample were drop-cast on a silicon wafer previously cleaned with isopropanol (ACS reagent, ≥ 99.5 %, Sigma-Aldrich) and dried with a nitrogen gun to avoid contamination. Samples were kept dry in a sealed box and analyzed the same day. Control samples were subject to the same procedure, and a plain silicon wafer was used as a procedural blank. Fiji (ImageJ version 1.53t, USA) software was used to include the scale bar in the SEM images and automatically calculate the size distribution of the particles.

### 2.6. Raman spectroscopy

Raman spectra of the new and used LDPE MPLs and their leachates were acquired using a WITec Alpha300R confocal Raman microscope (WITec) using a 532 nm laser line (5 mW, 5 s of time acquisition, 10 accumulations, 600 g/mm grating and using a 50× magnification air objective). Raman spectral data was extracted from the WITec Control 5 software provided by WITec and processed using GRAMS/AI™ spectroscopy software (ThermoFisher Scientific) to correct the baseline and cosmic ray removal. MPLs were placed in glass slides coated with aluminum foil due to the close-to-zero background of the foil, (Cui et al., 2016) whereas 5 μL of the different leachates were drop-cast onto a silicon wafer and analyzed when dried.

## 3. Results and discussion

To investigate the potential release of NPLs (particles <1 μm) into water from LDPE greenhouse cover films, small pieces (5 mm × 5 mm) of both new and used cover films (hereafter referred to as new-MPLs and used-MPLs) were immersed in Milli-Q water and subjected to simulated sunlight exposure for several days up to an equivalent of 6 months of real sunlight exposure. This period covers approximately from February to July, corresponding to the maturation of annual-cycle crops and the entire season of short-cycle spring crops, coinciding with the maximum hours of sunshine greenhouses receive. (Egea et al., 2021) The LDPE cover films used in the study were in field use for 3 years before being discarded for an unknown period and subsequently collected for analysis. It is worth noting that discarded plastics were obtained from the waste management company in the month following their withdrawal. Therefore, for comparative purposes, new-MPLs were exposed to simulated sunlight (irradiation; I) for 1, 3, 4, and 6 months, while used-MPLs were exposed for 4 and 6 months. Additionally, non-irradiated (NI) new-MPLs and used-MPLs (referred to as NI-new-MPLs and NI-used-MPLs) along with samples aged for 2 h in Milli-Q water without irradiation were included in the study as a control. A schematic representation of the experimental workflow is presented in Fig. 1.

After the simulated sunlight exposure, the leachates from both new-MPLs and used-MPLs were visualized using SEM to determine the presence of particles (Fig. 2A). Imaging was conducted at a low voltage under high vacuum conditions to ensure high-quality imaging without particle damage. In the irradiated new-MPLs (referred to as I-new-MPLs), well-defined spherical particles with an approximate diameter of ~200 nm were observed (Fig. 2C). In contrast, the irradiated used-MPLs (referred to as I-used-MPLs) exhibited particles with undefined shapes, and their size distribution could not be precisely determined. However, SEM images revealed particles smaller than 1 μm.

For the non-irradiated new-MPLs (NI-new-MPLs), particles with a diameter of ≤306 nm were visualized. The size of particles in the NI-new-MPLs-18d could not be measured due to challenging particle organization on the silicon wafer and the presence of large material (Figs. S1A and S1C). As well as for the I-used-MPLs, the size distribution of particles in the NI-used-MPLs could not be determined. Larger particles were observed in the control leachates, which were obtained from new-MPLs and used-MPs aged for 2 h without irradiation. Importantly, no features were observed in the silicon wafer used as a procedural blank, confirming the absence of cross-contamination during the sample preparation process (Fig. S2). Additional SEM images can be found in Fig. S2.

NTA, a non-destructive analytical technique, was employed to confirm the presence of particles smaller than 1 μm in the leachates (Figs. 2B and S1B), assess their size (i.e. distribution), and obtain the concentration of particles per mL. Leachates were analyzed without any pre-treatment step, except for those obtained from the used-MPLs and the NI-new-MPLs-18d, which were filtered using a 1 μm nylon membrane filter due to the presence of large-sized material. In line with SEM results, NTA reveals particles with an average size ≤238 nm (D90 ≤ 398 nm) for I-new-MPLs. Smaller particles were observed in leachates from the I-used-MPLs (average size ≤143 nm; D90 ≤ 198 nm, Fig. 2B and Table S1).

When comparing the number of particles/mL released from the I-MPLs (Fig. 2B and Table S1), it was interesting to observe that there was not a significant increment of particles within the months (i.e., simulated aging), neither in the I-new-MPLs nor in the I-used-MPLs, with the I-used-MPLs releasing higher amounts of particles than the I-new-MPLs.

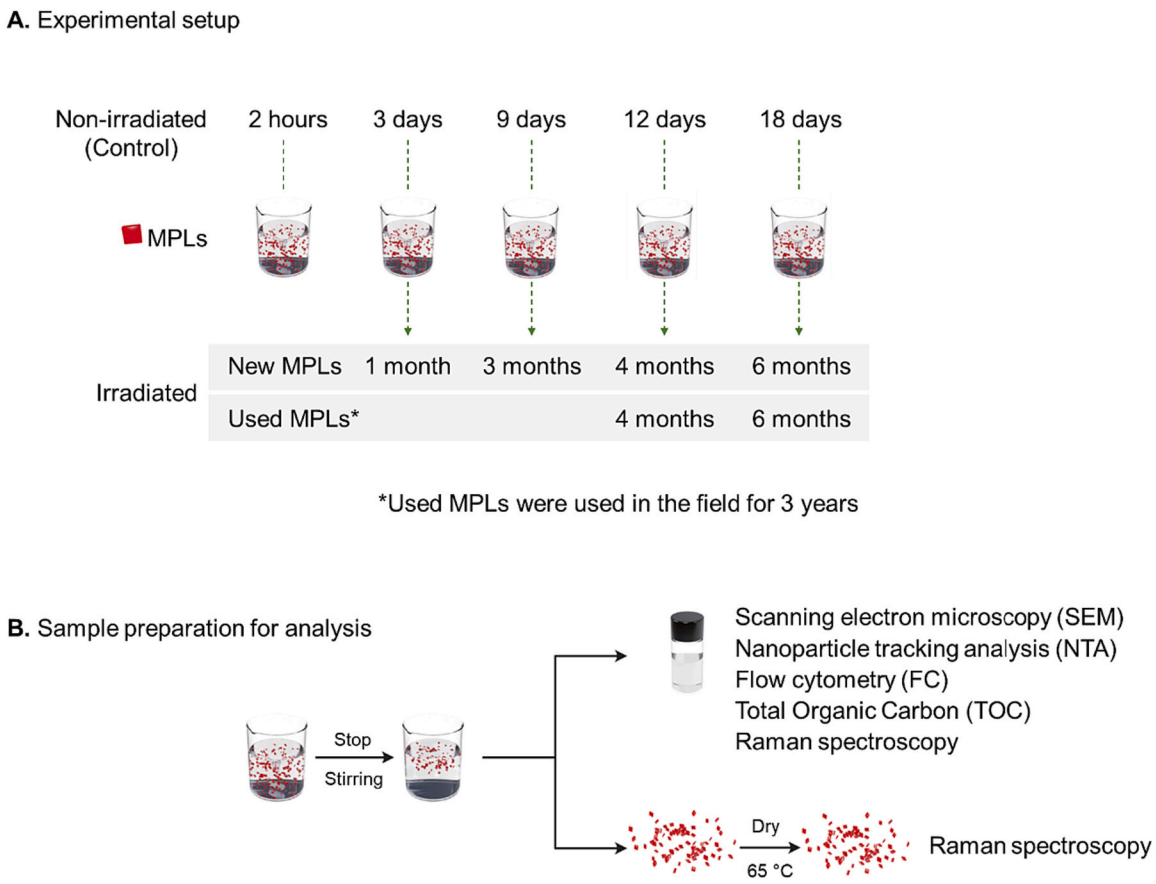


**Fig. 1. A.** Experimental workflow to study the presence of secondary MPLs and NPLs from LDPE MPLs under simulated sunlight exposure. **B.** Leachates were analyzed by SEM, NTA, FC, TOC, and Raman spectroscopy to characterize and quantify the presence of particles. Aged MPLs were also subject to Raman spectroscopy analysis.

However, the results confirm that greenhouse cover film releases nanoplastics not only after being discarded and disposed of into the environment but also during their everyday usage.

It is worth noting that the higher particle release from the I-used-MPLs compared to the I-new-MPLs cannot be solely attributed to secondary plastic particles. According to the literature, multi-layered LDPE greenhouse cover films contain various components such as mineral fillers, vinyl acetates like polyvinyl acetate (PVA) used as anti-fogging agents, or ethylene vinyl acetate (EVA) used as binders for the PE layers, metal-based pigments as additives to block NIR light, and UV absorbers, among others. (Dehbi et al., 2017) Therefore, additional nanomaterial could have been released during the simulated aging in both I-new-MPLs and I-used-MPLs, which is expected to be more predominant in the I-used-MPLs. Additionally, despite thoroughly cleaning the MPLs with Milli-Q water before simulated aging, it is possible that different materials remained attached to the MPLs and were subsequently released during the aging experiments.

Similar trends were observed for the NI-MPLs, with NI-used-MPLs releasing more particles/mL than NI-new-MPLs (Fig. S1B and Table S1). As for the I-MPLs, the particles released from the NI-used-MPLs are smaller than those released from the NI-new-MPLs. Interestingly, NTA shows no effect of photodegradation, i.e. irradiated vs non-irradiated MPLs, on the size and concentration of particles released from the new-MPLs and used-MPLs. Additionally, few particles in the same size range as those found in the leachates were present in the 2-h aged MPLs, confirming what was visualized in the SEM (Fig. S1B, Fig. 2B, and Table S1).

In addition to NTA, Flow Cytometry (FC) was employed to assess the presence of particles ranging from 1 μm up to 25 μm in the leachates (Fig. 3A and Table S2). For all size ranges, but more notably for the size fraction 1 μm – 5 μm, there was an increase in the number of particles per gram of PE (particles/gPE) over the months for the I-new-MPLs. The highest amount of particles was observed in the smallest size fraction, specifically 1 μm – 5 μm at each time point. These observations align with previous publications (Sorasan et al., 2021) that have demonstrated the degradation of secondary particles into smaller particles during aging leads to an increased quantity of particles in the smallest size fraction. Furthermore, the total number of particles in the I-new-MPLs, encompassing all particles with sizes $\leq$25 μm, increased over time (Fig. 3B and Table S2). No significant aging effects on the particles/gPE were observed by FC for the I-used-MPLs in all the size ranges (Fig. 3A and B and Table S2).

NI-new-MPLs showed a similar trend to I-new-MPLs, with particle/gPE increasing over the months, showing the highest significance for the size fraction 1 μm – 5 μm. The effect of photodegradation was evident and consistent, with I-new-MPLs releasing more particles than NI-new-MPLs at each time point (Fig. 3, Fig. S3, and Table S2). A slight effect of aging was observed for the NI-used-MPLs, which released a slightly higher amount of particles/gPE at 18 days than at 12 days (Figs. S3A and S3B). No effects of photodegradation were observed when comparing the particles/gPE released from the I-used-MPLs and NI-used-MPLs (Fig. 3, Fig. S3, and Table S2).

Additional results obtained by FC and expressed as milligram particles per gram of PE (mgParticles/gPE) are consistent with the data expressed as the number of particles/gPE, showing I-new-MPLs releasing more mgParticles/gPE than I-used-MPLs (Fig. 3C), and a clear effect of photodegradation only for new-MPLs (Fig. 3C, Fig. S3C, and Table S2). Interestingly, the total number of particles/gPE and the

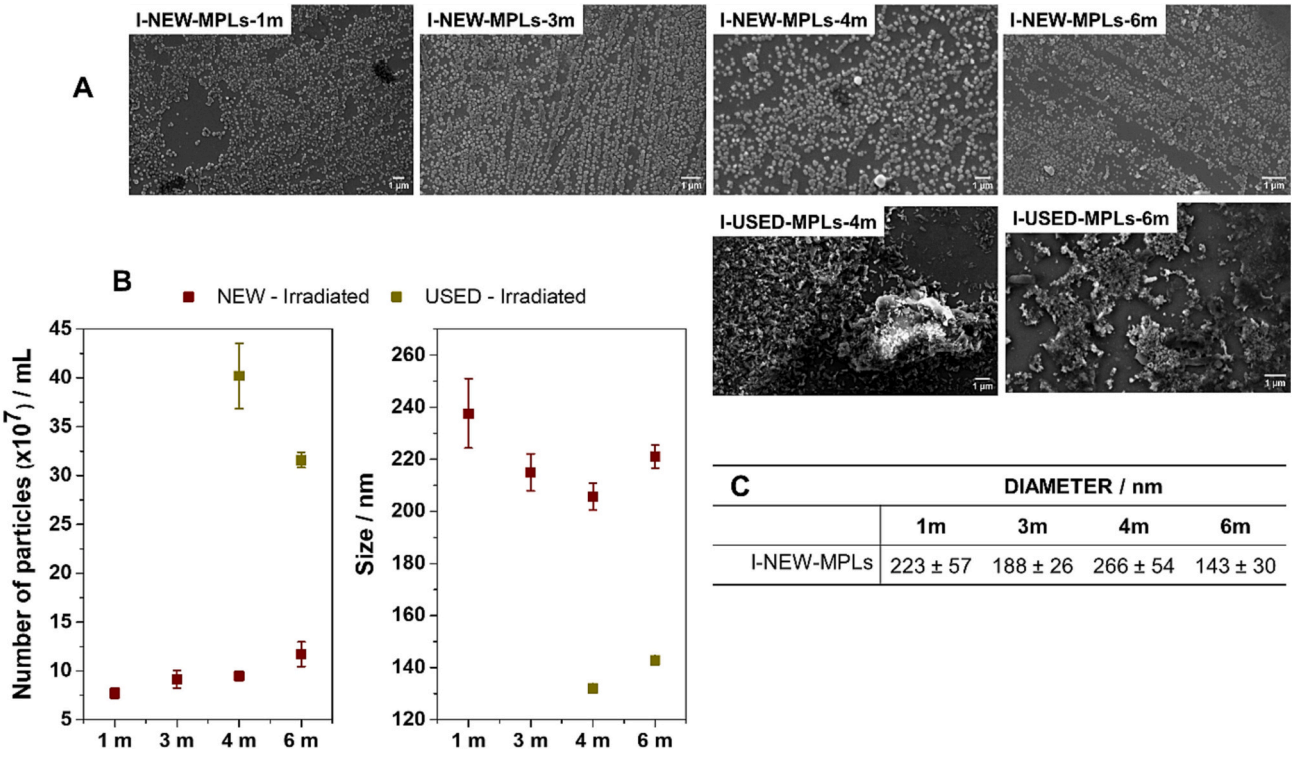


C

| | DIAMETER / nm | | | |
|---|---|---|---|---|
| | 1m | 3m | 4m | 6m |
| I-NEW-MPLs | 223 ± 57 | 188 ± 26 | 266 ± 54 | 143 ± 30 |

**Fig. 2. A.** SEM micrographs showing particles with diameters <1 μm released from the I-new-MPLs and I-used-MPLs. Scale bar: 1 μm. **B.** Concentration and size of the particles released from the I-new-MPLs and I-used-MPLs obtained by NTA at different aging times. Error bars represent the standard deviation obtained from recording five videos of 60 s each. **C.** The Inset table summarizes the diameter of the particles calculated from SEM images using Fiji software for the I-new-MPLs.

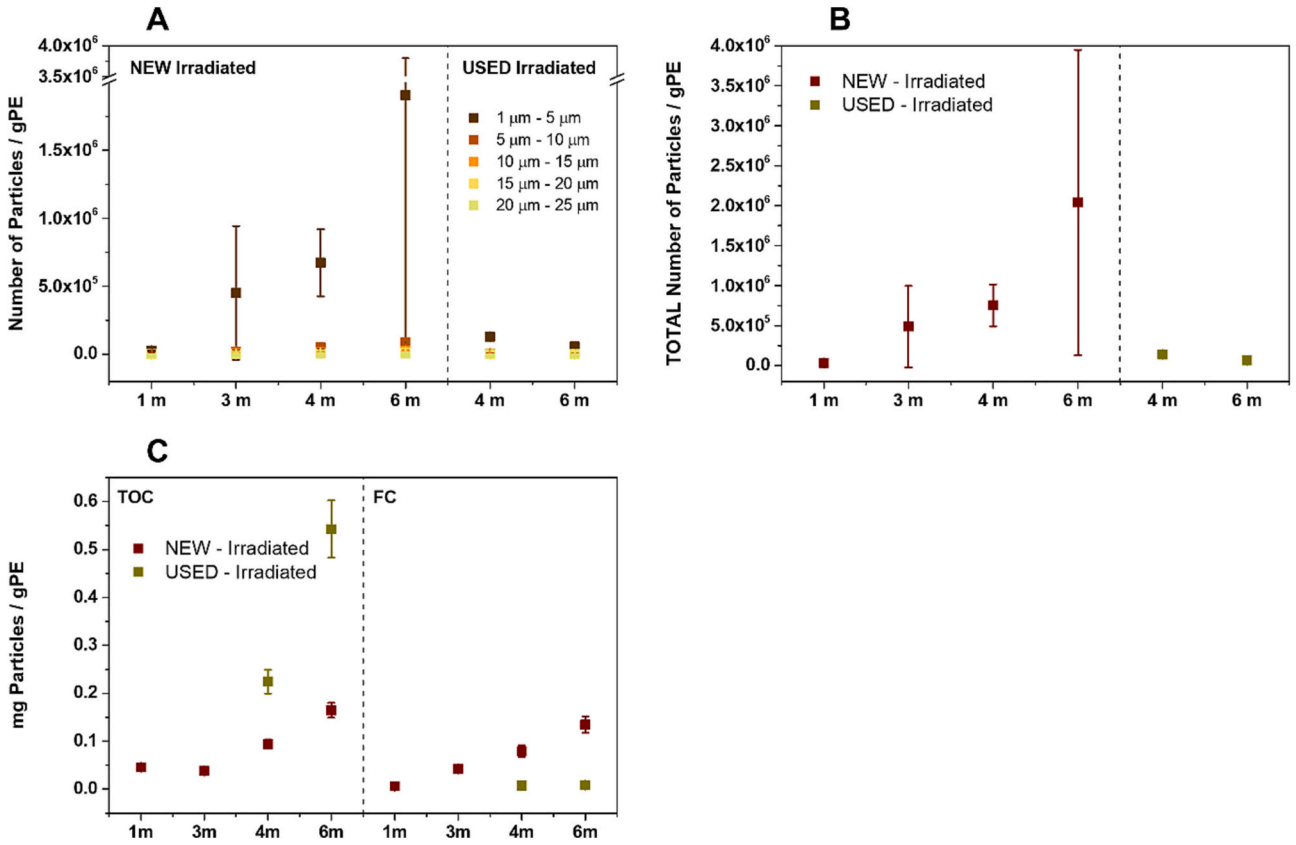


**Fig. 3. A.** Concentration of particles in the leachates obtained by FC expressed as the number of particles per gPE for I-new-MPLs and I-used-MPLs. **B.** Total concentration of particles in the leachates obtained by FC expressed as the number of particles per gPE. **C.** Total carbon in the leachates for the new-MPLs and used-MPLs measured by TOC analyzer and FC. The mg Particles/g PE was calculated following the procedure described elsewhere (Sorasan et al., 2021).

mgParticles/gPE obtained by FC for the I-used-MPLs (Fig. 3C) at 4 and 6 months was comparable to the NI-used-MPLs and the NI-new-MPLs (Fig. S3C) at 12 and 18 days. This result suggests that I-used-MPLs, NI-used-MPLs, and NI-new-MPLs behave similarly in terms of the release of secondary microparticles.

Complementary values corresponding to the total carbon present in the leachates (Fig. 3C and Fig. S3C) demonstrated an influence of simulated aging for both I-new-MPLs and I-used-MPLs, with the I-used-MPLs releasing a higher amount of mgParticles/gPE compared to the I-new-MPLs. When comparing the results from FC and TOC, TOC showed higher values in mgParticles/gPE than those from FC at each time point, indicating that material with a chemical composition different from PE was released during the aging process.

Lastly, data obtained from FC regarding the release of secondary microparticles (Fig. 3 and Fig. S3), along with data concerning the release of secondary nanoparticles (NTA, Fig. 2B, and S1B), provide evidence that the release of micro- and nanoparticles under irradiation follows distinct trends. In the case of nanoparticle release, no discernible influence of simulated aging was observed for both new and used cover films. In contrast, an effect of natural aging was apparent, with I-used-MPLs releasing more nanoparticles than I-new-MPLs. Conversely, the release of microparticles is influenced by both simulated and the natural aging of the cover films.

Chemical analysis of the cover films and leachates was performed by Raman spectroscopy using a 532 nm laser line to evaluate if the nanoparticles released from the MPLs correspond to nanoPE, i.e., NPLs of PE. Control leachates were also analyzed. For clarity of comparison, the Raman spectra of the as-received films were also included (Figs. 4, S4, S5, and S6).

As shown in Fig. S4, the new and used as-received films display similar Raman fingerprint involving the characteristic peaks related to PE: peaks centered at 1296 $cm^{-1}$, 1418 $cm^{-1}$, 1442 $cm^{-1}$, 1460 $cm^{-1}$, 2848 $cm^{-1}$, and 2881 $cm^{-1}$, being of more relevance for this study the bands at 1296 $cm^{-1}$ non-crystalline consecutive trans and at 1418 $cm^{-1}$

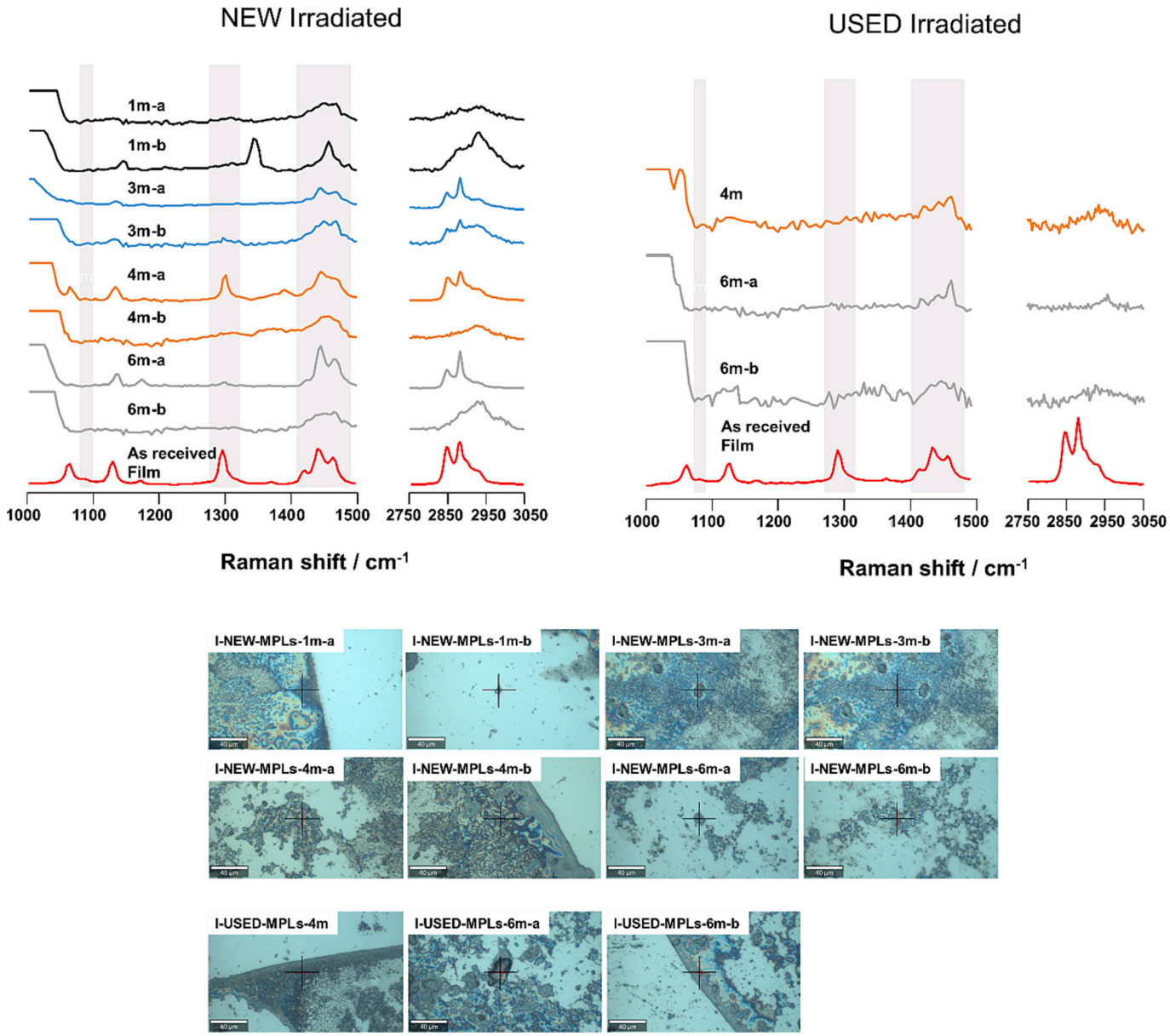


**Fig. 4.** Raman spectra for the leachates from I-new-MPLs and I-used-MPLs were acquired using a 532 nm laser line at different aging times. Several spots were analyzed for all the samples showing low-crystalline PE NPLs. Bright-field images showing the different spots where the Raman spectra were recorded in the leachates for the new-MPLs and used-MPLs at different aging times. Scale bar: 40 μm.

characteristic of the orthorhombic crystalline phase; 1442 $cm^{-1}$ and 1460 $cm^{-1}$ characteristic of an amorphous phase. A broad band at 1083 $cm^{-1}$ associated with an amorphous phase was also found in both new and used as-received films. (Jin et al., 2017; Sato et al., 2002) A table summarizing all the Raman shift assignments was included in Table S3.

In all leachates from the new-MPLs, very low crystalline nanoPE was found independent of the irradiation time. Particles with sizes above 1 μm (Fig. 4 spectra and bright-field images corresponding to I-new-I-1 m-b, I-new-3 m-a, I-new-6 m-a), were found to be more crystalline than nanoPE in both leachates from I-new-MPLs and NI-new-MPLs (Fig. S5, NI-new-4 m-b, NI-new-6 m-b, I-used-6 m-a, NI-used-4 m-b). The loss in crystallinity can be evaluated by the decrease in intensity of the Raman peaks, especially the peak at 1296 $cm^{-1}$, and the broadness of the peaks in the regions 1400 $cm^{-1}$–1500 $cm^{-1}$ and 2750 $cm^{-1}$–2950 $cm^{-1}$.(Jin et al., 2017; Samuel et al., 2017; Sato et al., 2002) Similar results were found for the I-used-MPLs (Fig. 4). The nanoPE found in the leachates from I-used-MPLs and NI-used-MPLs shows a low degree of crystallinity upon irradiation compared to new-MPLs. PE particles with low crystallinity were also found in the control samples from new-MPLs and used-MPLs.

The 5 mm × 5 mm new-MPLs and used-MPLs were also investigated by Raman spectroscopy using a 532 nm laser line (Fig. S6), and the spectra obtained correspond to LDPE. In this study, the effect of the photooxidation on the crystallinity of the MPLs was not assessed as degradation is expected not to be uniform, i.e., portions of the MPLs might be more affected by the irradiation than others. However, few authors have already reported the effects of aging on LDPE MPLs, showing that upon weathering, the amorphous phase is preferentially degraded over the crystalline phase resulting in more crystalline MPLs. (Andrady, 2017; Hiejima et al., 2018; Phan et al., 2022) These studies may also support our findings concerning the low-crystalline nanoPE detected in the leachates.

## 4. Conclusions

In this study, we reported the presence of nanoPE (NPLs of PE) released to water during the simulated aging of LDPE greenhouse cover films as microplastics over a typical six-month vegetable growth period in Almeria, Spain. Notably, the released nanoPE exhibited a lower degree of crystallinity compared to the initial MPLs. Findings from FC, NTA, and TOC analyses indicated that materials other than PE were released during the aging process, with irradiation impacting only the release of microplastics in the new cover films. Furthermore, our study provides evidence that new and naturally aged plastics exhibit different behaviors in terms of micro- and nanoplastic release. Importantly, our data emphasize the significance of using multiple techniques to analyze the presence of secondary MPLs and NPLs resulting from the degradation of larger plastics. The study also underscores the importance of investigating the release of MPLs and NPLs in both new and naturally aged (used) materials.

## CRediT authorship contribution statement

**Carmen Sorasan:** Methodology, Investigation. **Patricia Taladriz-Blanco:** Writing – review & editing, Writing – original draft, Validation, Supervision, Methodology, Investigation, Formal analysis. **Laura Rodriguez-Lorenzo:** Writing – review & editing, Supervision, Resources. **Begoña Espiña:** Writing – review & editing, Resources, Funding acquisition. **Roberto Rosal:** Writing – review & editing, Validation, Funding acquisition, Conceptualization.

## Declaration of competing interest

The authors declare that they have no known competing financial interests or personal relationships that could have appeared to influence the work reported in this paper.

## Data availability

Data will be made available on request.

## Acknowledgments

P.T—B, L.R-L, and B.E acknowledge funding from the LABPLAS Project (LAnd-Based Solutions for PLAStics in the Sea, Grant Agreement Nr.: 101003954, financed by the EU H2020 program), SbDtoolBox - Nanotechnology-based tools and tests for Safer-by-Design nanomaterials, with the reference n.° NORTE-01-0145-FEDER-000047, funded by Norte2020 – North-Regional Operational Programme under the PORTUGAL 2020 Partnership Agreement, through the European Regional Development Fund (ERDF). L.R.-L. acknowledges also funding to FCT (Fundação para a Ciência e Tecnologia) for the Scientific Employment Stimulus Program (2020.04021.CEECIND). The authors acknowledge Dr. Jessica Caldwell for proof-reading the manuscript and to Dr. Miguel Spuch-Calvar for creating the graphical abstract artwork.

## Appendix A. Supplementary data

Supplementary data to this article can be found online at https://doi.org/10.1016/j.scitotenv.2024.170662.

## References

Alimi, O.S., Farner Budarz, J., Hernandez, L.M., Tufenkji, N., 2018. Microplastics and Nanoplastics in aquatic environments: aggregation, deposition, and enhanced contaminant transport. Environ. Sci. Technol. 52, 1704–1724. https://doi.org/10.1021/acs.est.7b05559.

Allen, D., Allen, S., Abbasi, S., Baker, A., Bergmann, M., Brahney, J., Butler, T., Duce, R. A., Eckhardt, S., Evangeliou, N., Jickells, T., Kanakidou, M., Kershaw, P., Laj, P., Levermore, J., Li, D., Liss, P., Liu, K., Mahowald, N., Masque, P., Materić, D., Mayes, A.G., McGinnity, P., Osvath, I., Prather, K.A., Prospero, J.M., Revell, L.E., Sander, S.G., Shim, W.J., Slade, J., Stein, A., Tarasova, O., Wright, S., 2022. Microplastics and nanoplastics in the marine-atmosphere environment. Nat. Rev. Earth Environ. 3, 393–405. https://doi.org/10.1038/s43017-022-00292-x.

Andrady, A.L., 2017. The plastic in microplastics: a review. Mar. Pollut. Bull. 119, 12–22. https://doi.org/10.1016/j.marpolbul.2017.01.082.

Astner, A.F., Gillmore, A.B., Yu, Y., Flury, M., DeBruyn, J.M., Schaeffer, S.M., Hayes, D. G., 2023. Formation, behavior, properties and impact of micro- and nanoplastics on agricultural soil ecosystems (a review). NanoImpact 31, 100474. https://doi.org/10.1016/j.impact.2023.100474.

Belz, S., Bianchi, I., Cella, C., Emteborg, H., Fumagalli, F., Geiss, O., Gilliland, D., Held, A., Jakobsson, U., La Spina, R., Mėhn, D.R.Y., Robouch, P., Seghers, J., Sokull-Kluettgen, B., Stefaniak, E., Stroka, J., 2021. Current status of the quantification of microplastics in water: results of a JRC/BAM interlaboratory comparison study on PET in wate. EUR 30799 EN. Publ. Off. Eur. Union. https://doi.org/10.2760/27641.

Caldwell, J., Taladriz-Blanco, P., Rothen-Rutishauser, B., Petri-Fink, A., 2021. Detection of sub-micro- and nanoplastic particles on gold nanoparticle-based substrates through surface-enhanced Raman scattering (SERS) spectroscopy. Nanomaterials 11, 1149. https://doi.org/10.3390/nano11051149.

Caldwell, J., Taladriz-Blanco, P., Lehner, R., Lubskyy, A., Ortuso, R.D., Rothen-Rutishauser, B., Petri-Fink, A., 2022. The micro-, submicron-, and nanoplastic hunt: a review of detection methods for plastic particles. Chemosphere 293, 133514. https://doi.org/10.1016/j.chemosphere.2022.133514.

Castillo-Díaz, F.J., Belmonte-Ureña, L.J., Camacho-Ferre, F., Tello-Marquina, J.C., 2021. The management of agriculture plastic waste in the framework of circular economy. case of the Almeria Greenhouse (Spain). Int. J. Environ. Res. Public Health. https://doi.org/10.3390/ijerph182212042.

Chamas, A., Moon, H., Zheng, J., Qiu, Y., Tabassum, T., Jang, J.H., Abu-Omar, M., Scott, S.L., Suh, S., 2020. Degradation rates of plastics in the environment. ACS Sustain. Chem. Eng. 8, 3494–3511. https://doi.org/10.1021/acssuschemeng.9b06635.

Cui, L., Butler, H.J., Martin-Hirsch, P.L., Martin, F.L., 2016. Aluminium foil as a potential substrate for ATR-FTIR, transflection FTIR or Raman spectrochemical analysis of biological specimens. Anal. Methods 8, 481–487. https://doi.org/10.1039/C5AY02638E.

Cui, Q., Yang, X., Li, J., Miao, Y., Zhang, X., 2022. Microplastics generation behavior of polypropylene films with different crystalline structures under UV irradiation. Polym. Degrad. Stab. 199, 109916 https://doi.org/10.1016/j.polymdegradstab.2022.109916.

Dehbi, A., Youssef, B., Chappey, C., Mourad, A.-H.I., Picuno, P., Statuto, D., 2017. Multilayers polyethylene film for crop protection in harsh climatic conditions. Adv. Mater. Sci. Eng. 2017, 4205862. https://doi.org/10.1155/2017/4205862.

EFSA CONTAM Panel (EFSA Panel on Contaminants in the Food Chain), 2016. Statement on the presence of microplastics and nanoplastics in food, with particular focus on seafood. EFSA J. 14, 4501. https://doi.org/10.2903/j.efsa.2016.4501.

Egea, F.J., López-Rodríguez, M.D., Oña-Burgos, P., Castro, A.J., Glass, C.R., 2021. Bioeconomy as a transforming driver of intensive greenhouse horticulture in SE Spain. N. Biotechnol. 61, 50–56. https://doi.org/10.1016/j.nbt.2020.11.010.

Ekvall, M.T., Lundqvist, M., Kelpsiene, E., Šileikis, E., Gunnarsson, S.B., Cedervall, T., 2019. Nanoplastics formed during the mechanical breakdown of daily-use polystyrene products. Nanoscale Adv. 1, 1055–1061. https://doi.org/10.1039/C8NA00210J.

Filipe, V., Hawe, A., Jiskoot, W., 2010. Critical evaluation of nanoparticle tracking analysis (NTA) by NanoSight for the measurement of nanoparticles and protein aggregates. Pharm. Res. 27, 796–810. https://doi.org/10.1007/s11095-010-0073-2.

Gálvez-Blanca, V., Edo, C., González-Pleiter, M., Albentosa, M., Bayo, J., Beiras, R., Fernández-Piñas, F., Gago, J., Gómez, M., Gonzalez-Cascon, R., Hernández-Borges, J., Landaburu-Aguirre, J., Martínez, I., Muniategui-Lorenzo, S., Romera-Castillo, C., Rosal, R., 2023. Occurrence and size distribution study of microplastics in household water from different cities in continental Spain and the Canary Islands. Water Res. 238, 120044 https://doi.org/10.1016/j.watres.2023.120044.

Gigault, J., Pedrono, B., Maxit, B., Ter Halle, A., 2016. Marine plastic litter: the unanalyzed nano-fraction. Environ. Sci. Nano 3, 346–350. https://doi.org/10.1039/C6EN00008H.

Gigault, J., ter Halle, A., Baudrimont, M., Pascal, P.-Y., Gauffre, F., Phi, T.-L., El Hadri, H., Grassl, B., Reynaud, S., 2018. Current opinion: what is a nanoplastic? Environ. Pollut. 235, 1030–1034. https://doi.org/10.1016/j.envpol.2018.01.024.

Gigault, J., El Hadri, H., Nguyen, B., Grassl, B., Rowenczyk, L., Tufenkji, N., Feng, S., Wiesner, M., 2021. Nanoplastics are neither microplastics nor engineered nanoparticles. Nat. Nanotechnol. 16, 501–507. https://doi.org/10.1038/s41565-021-00886-4.

González-Pleiter, M., Tamayo-Belda, M., Pulido-Reyes, G., Amariei, G., Leganés, F., Rosal, R., Fernández-Piñas, F., 2019. Secondary nanoplastics released from a biodegradable microplastic severely impact freshwater environments. Environ. Sci. Nano 6, 1382–1392. https://doi.org/10.1039/C8EN01427B.

Gündoğdu, R., Önder, D., Gündoğdu, S., Gwinnett, C., 2022b. Plastics derived from disposable greenhouse plastic films and irrigation pipes in agricultural soils: a case study from Turkey. Environ. Sci. Pollut. Res. 29, 87706–87716. https://doi.org/10.1007/s11356-022-21911-6.

Gündoğdu, S., Ayat, B., Aydoğan, B., Çevik, C., Karaca, S., 2022a. Hydrometeorological assessments of the transport of microplastic pellets in the Eastern Mediterranean. Sci. Total Environ. 823, 153676 https://doi.org/10.1016/j.scitotenv.2022.153676.

Hartmann, N.B., Hüffer, T., Thompson, R.C., Hassellöv, M., Verschoor, A., Daugaard, A. E., Rist, S., Karlsson, T., Brennholt, N., Cole, M., Herrling, M.P., Hess, M.C., Ivleva, N. P., Lusher, A.L., Wagner, M., 2019. Are we speaking the same language? Recommendations for a definition and categorization framework for plastic debris. Environ. Sci. Technol. 53, 1039–1047. https://doi.org/10.1021/acs.est.8b05297.

Hernandez, L.M., Xu, E.G., Larsson, H.C.E., Tahara, R., Maisuria, V.B., Tufenkji, N., 2019. Plastic teabags release billions of microparticles and nanoparticles into tea. Environ. Sci. Technol. 53, 12300–12310. https://doi.org/10.1021/acs.est.9b02540.

Hiejima, Y., Kida, T., Takeda, K., Igarashi, T., Nitta, K., 2018. Microscopic structural changes during photodegradation of low-density polyethylene detected by Raman spectroscopy. Polym. Degrad. Stab. 150, 67–72. https://doi.org/10.1016/j.polymdegradstab. 2018.02.010.

Hitchcock, J.N., 2020. Storm events as key moments of microplastic contamination in aquatic ecosystems. Sci. Total Environ. 734, 139436 https://doi.org/10.1016/j.scitotenv.2020.139436.

Ivleva, N.P., 2021. Chemical analysis of microplastics and nanoplastics: challenges, advanced methods, and perspectives. Chem. Rev. 121, 11886. https://doi.org/10.1021/acs.chemrev.1c00178.

Ivleva, N.P., Wiesheu, A.C., Niessner, R., 2017. Microplastic in aquatic ecosystems. Angew. Chem. Int. Ed. 56, 1720–1739. https://doi.org/10.1002/anie.201606957.

Jin, Y., Kotula, A.P., Snyder, C.R., Hight Walker, A.R., Migler, K.B., Lee, Y.J., 2017. Raman identification of multiple melting peaks of polyethylene. Macromolecules 50, 6174–6183. https://doi.org/10.1021/acs.macromol.7b01055.

Kihara, S., Chan, A., In, E., Taleb, N., Tollemache, C., Yick, S., McGillivray, D.J., 2022. Detecting polystyrene nanoplastics using filter paper-based surface-enhanced Raman spectroscopy. RSC Adv. 12, 20519–20522. https://doi.org/10.1039/D2RA03395J.

Li, K., Xiu, X., Hao, W., 2024. Microplastics in soils: production, behavior process, impact on soil organisms, and related toxicity mechanisms. Chemosphere 350, 141060. https://doi.org/10.1016/j.chemosphere.2023.141060.

Liu, L., Xu, M., Ye, Y., Zhang, B., 2022. On the degradation of (micro)plastics: degradation methods, influencing factors, environmental impacts. Sci. Total Environ. 806, 151312 https://doi.org/10.1016/j.scitotenv.2021.151312.

Lv, L., He, L., Jiang, S., Chen, J., Zhou, C., Qu, J., Lu, Y., Hong, P., Sun, S., Li, C., 2020. In situ surface-enhanced Raman spectroscopy for detecting microplastics and nanoplastics in aquatic environments. Sci. Total Environ. 728, 138449 https://doi.org/10.1016/j.scitotenv.2020.138449.

Mehrabi, K., Nowack, B., Arroyo Rojas Dasilva, Y., Mitrano, D.M., 2017. Improvements in nanoparticle tracking analysis to measure particle aggregation and mass distribution: a case study on engineered nanomaterial stability in incineration landfill leachates. Environ. Sci. Technol. 51, 5611–5621. https://doi.org/10.1021/acs.est.7b00597.

Mitrano, D.M., Wick, P., Nowack, B., 2021. Placing nanoplastics in the context of global plastic pollution. Nat. Nanotechnol. 16, 491–500. https://doi.org/10.1038/s41565-021-00888-2.

Science for the Environment Policy, 2023. Nanoplastics: state of knowledge and environmental and human health impacts. Future Brief (27). Brief produced for the European Commision DG Environmental by the Science Communication Unit, UWE Bristol. https://ec.europa.eu/science-environment-policy.

Owusu, S.M., Adomako, M.O., Qiao, H., 2024. Organic amendment in climate change mitigation: challenges in an era of micro- and nanoplastics. Sci. Total Environ. 907, 168035 https://doi.org/10.1016/j.scitotenv.2023.168035.

Pérez-Reverón, R., Álvarez-Méndez, S.J., González-Sálamo, J., Socas-Hernández, C., Díaz-Peña, F.J., Hernández-Sánchez, C., Hernández-Borges, J., 2023. Nanoplastics in the soil environment: analytical methods, occurrence, fate and ecological implications. Environ. Pollut. 317, 120788 https://doi.org/10.1016/j.envpol.2022.120788.

Pfohl, P., Wagner, M., Meyer, L., Domercq, P., Praetorius, A., Hüffer, T., Hofmann, T., Wohlleben, W., 2022. Environmental degradation of microplastics: how to measure fragmentation rates to secondary micro- and nanoplastic fragments and dissociation into dissolved organics. Environ. Sci. Technol. 56, 11323–11334. https://doi.org/10.1021/acs.est.2c01228.

Phan, S., Padilla-Gamiño, J.L., Luscombe, C.K., 2022. The effect of weathering environments on microplastic chemical identification with Raman and IR spectroscopy: part I. Polyethylene and polypropylene. Polym. Test. 116, 107752 https://doi.org/10.1016/j.polymertesting.2022.107752.

Samuel, A.Z., Lai, B.-H., Lan, S.-T., Ando, M., Wang, C.-L., Hamaguchi, H., 2017. Estimating percent crystallinity of polyethylene as a function of temperature by Raman spectroscopy multivariate curve resolution by alternating least squares. Anal. Chem. 89, 3043–3050. https://doi.org/10.1021/acs.analchem.6b04750.

Sato, H., Shimoyama, M., Kamiya, T., Amari, T., Šašic, S., Ninomiya, T., Siesler, H.W., Ozaki, Y., 2002. Raman spectra of high-density, low-density, and linear low-density polyethylene pellets and prediction of their physical properties by multivariate data analysis. J. Appl. Polym. Sci. 86, 443–448. https://doi.org/10.1002/app.10999.

Sharma, S., Sharma, V., Chatterjee, S., 2023. Contribution of plastic and microplastic to global climate change and their conjoining impacts on the environment - a review. Sci. Total Environ. 875, 162627 https://doi.org/10.1016/j.scitotenv.2023.162627.

Song, Y.K., Hong, S.H., Eo, S., Han, G.M., Shim, W.J., 2020. Rapid production of micro- and nanoplastics by fragmentation of expanded polystyrene exposed to sunlight. Environ. Sci. Technol. 54, 11191–11200. https://doi.org/10.1021/acs.est.0c02288.

Song, Y.K., Hong, S.H., Eo, S., Shim, W.J., 2022. The fragmentation of nano- and microplastic particles from thermoplastics accelerated by simulated-sunlight-mediated photooxidation. Environ. Pollut. 311, 119847 https://doi.org/10.1016/j.envpol.2022.119847.

Sorasan, C., Edo, C., González-Pleiter, M., Fernández-Piñas, F., Leganés, F., Rodríguez, A., Rosal, R., 2021. Generation of nanoplastics during the photoageing of low-density polyethylene. Environ. Pollut. 289, 117919 https://doi.org/10.1016/j.envpol.2021.117919.

Sorasan, C., Edo, C., González-Pleiter, M., Fernández-Piñas, F., Leganés, F., Rodríguez, A., Rosal, R., 2022. Ageing and fragmentation of marine microplastics. Sci. Total Environ. 827, 154438 https://doi.org/10.1016/j.scitotenv.2022.154438.

de Souza Machado, A.A., Lau, C.W., Kloas, W., Bergmann, J., Bachelier, J.B., Faltin, E., Becker, R., Görlich, A.S., Rillig, M.C., 2019. Microplastics can change soil properties and affect plant performance. Environ. Sci. Technol. 53, 6044–6052. https://doi.org/10.1021/acs.est.9b01339.

Tong, H., Zhong, X., Duan, Z., Yi, X., Cheng, F., Xu, W., Yang, X., 2022. Micro- and nanoplastics released from biodegradable and conventional plastics during degradation: formation, aging factors, and toxicity. Sci. Total Environ. 833, 155275 https://doi.org/10.1016/j.scitotenv.2022.155275.

Wang, C., Chen, W., Zhao, H., Tang, J., Li, G., Zhou, Q., Sun, J., Xing, B., 2023. Microplastic Fiber release by laundry: a comparative study of hand-washing and machine-washing. ACS ES&T Water 3, 147–155. https://doi.org/10.1021/acsestwater.2c00462.

Zhang, K., Hamidian, A.H., Tubić, A., Zhang, Y., Fang, J.K.H., Wu, C., Lam, P.K.S., 2021. Understanding plastic degradation and microplastic formation in the environment: a review. Environ. Pollut. 274, 116554 https://doi.org/10.1016/j.envpol.2021.116554.